

On the association between helical flow and plaque progression in coronary arteries

G. De Nisco¹, A. Hoogendoorn², A.M. Kok², C. Chiastra¹, D. Gallo¹,
U. Morbiducci¹, and J.J. Wentzel²

¹ PoliTo^{BIO}Med Lab, Department of Mechanical and Aerospace Engineering, Politecnico di Torino, Turin, Italy

² Department of Biomedical Engineering, ErasmusMC, Rotterdam, The Netherlands

Abstract— Arterial hemodynamics is markedly characterized by the presence of helical flow (HF) patterns, whose physiological significance has been investigated in recent years, in particular with respect to the atheroprotective role played by specific HF structures. However, a gap in knowledge still exist on the significance of HF in coronary arteries, a prominent site of atherosclerotic plaque formation.

The aim of this study is to carry out, in a representative sample of 15 swine coronary arteries, a systematic analysis of HF and wall thickness using computational fluid dynamics and intravascular ultrasound imaging. In detail, here we investigate possible associations of HF with (1) atherogenic wall shear stress (WSS) phenotypes, and (2) atherosclerotic plaque progression (in a follow up study). Our findings demonstrate for the first time that: (1) HF naturally characterizes coronary hemodynamics; (2) unfavourable conditions of WSS are strongly inversely associated with helicity intensity; (3) HF intensity protects against atherosclerotic plaque growth.

Keywords—atherosclerosis, WSS, helical flow, plaque growth.

I. INTRODUCTION

IT has been suggested that HF (1) protects from atherosclerosis by mitigating flow disturbances in human arteries [1], and (2) an inverse association with atherosclerosis at the early stage has been observed [2]. Challenged by the physiological significance of HF in the arterial system, here we investigate for the first time, the existence of a link between HF and disturbed shear, and HF and wall thickness (WT) in a follow up study, in a representative sample of swine-specific computational models of coronary arteries. The ultimate goal is exploring the significance of HF in coronary artery and its potency in predicting plaque growth.

II. MATERIALS AND METHODS

Five adult hypercholesterolemic pigs were put on a high fat diet and underwent computed tomography (CT) angiography and intravascular ultrasound (IVUS) imaging of the three main coronary arteries at two time points (baseline - after 3 months since start of the diet; T2 - after 9.4±1.9 months). The lumen geometry of 15 imaged coronary arteries (5 left anterior descending - LAD, 5 left circumflex - LCX, and 5 right coronary arteries - RCA) was reconstructed at baseline [3]. Transient computational fluid dynamics simulations were performed by using the finite volume method. Blood was modelled as non-Newtonian Carreau fluid. Personalized inflow and outflow boundary conditions were derived from Doppler flow velocity measurements by applying the scaling law proposed elsewhere [4].

Hemodynamic descriptors

Three descriptors of low/oscillatory WSS, i.e. time-averaged WSS (TAWSS), oscillatory shear index (OSI), and relative residence time (RRT) were computed (Table I). Additionally, the following two descriptors quantifying WSS multidirectionality were considered (Table I): transverse WSS (transWSS), representing the time-averaged WSS component orthogonal to the cycle-averaged direction of WSS vector [5], and its normalized counterpart cross-flow index (CFI). Data from all cases were combined to define objective thresholds for ‘disturbed flow’: the upper (lower) 33th percentile was identified for OSI, RRT, transWSS and CFI (TAWSS) [6]. For each model, the percentage of luminal area exposed to TAWSS values lower (higher for the other descriptors) than the defined thresholds was quantified and respectively labeled as TAWSS33, OSI66, RRT66, transWSS66, and CFI66.

TABLE I
NEAR-WALL AND INTRAVASCULAR HEMODYNAMIC DESCRIPTORS

TAWSS	$\text{TAWSS} = \frac{1}{T} \int_0^T \mathbf{WSS} dt$
OSI	$\text{OSI} = 0.5 \left[1 - \frac{\left \int_0^T \mathbf{WSS} dt \right }{\int_0^T \mathbf{WSS} dt} \right]$
RRT	$\text{RRT} = \frac{1}{\frac{1}{T} \int_0^T \mathbf{WSS} dt}$
transWSS	$\text{transWSS} = \frac{1}{T} \int_0^T \left \mathbf{WSS} \cdot \left(\mathbf{n} \times \frac{\int_0^T \mathbf{WSS} dt}{\int_0^T \mathbf{WSS} dt} \right) \right dt$
CFI	$\text{CFI} = \frac{1}{T} \int_0^T \frac{\mathbf{WSS}}{ \mathbf{WSS} } \cdot \left(\mathbf{n} \times \frac{\int_0^T \mathbf{WSS} dt}{\int_0^T \mathbf{WSS} dt} \right) dt$
h_2	$h_2 = \frac{1}{TV} \int_0^T \int_V \mathbf{v} \cdot \boldsymbol{\omega} dV dt$
LNH	$\text{LNH} = \frac{\mathbf{v} \cdot \boldsymbol{\omega}}{ \mathbf{v} \cdot \boldsymbol{\omega} } = \cos \gamma$

WSS is the WSS vector; T is the period of the cardiac cycle; V is the model volume; \mathbf{n} is the unit vector normal to the arterial surface at each element; \mathbf{v} is the velocity vector; $\boldsymbol{\omega}$ is the vorticity vector.

Intravascular hemodynamics was investigated in terms of cycle-average helicity intensity (h_2 , Table I) [2]. Additionally, local normalized helicity (LNH) was used to visualize intravascular HF structures (Table I) [1].

Wall thickness vs. helicity analysis

The analysis was focused on the IVUS imaged arterial segments, because of the higher accuracy in WT measurement. Each IVUS imaged arterial segment was divided into 3mm/45°

sector. h_2 in the whole volume and in the near-wall region (outer 10% of the local radius) was cycle- and volume-averaged over each 3mm/45° sector. WT was evaluated by subtracting the distance from the lumen centre of the outer and inner (segmented) wall boundaries. The mean values of the difference between T2 and baseline WT measurements was evaluated for each sector and normalized to follow-up time (Δ WT/month). Helicity data were divided into artery-specific tertiles (low, mid and high) to perform a statistical analysis using a linear mixed effects model. Significance was assumed for $p < 0.05$.

III. RESULTS

HF patterns were visualized using cycle-average LNH isosurfaces (Fig. 1). Notably, all 15 coronary artery models presented two distinguishable counter-rotating HF structures distributed all along the length of the artery, although with different intensity. No marked difference among coronary artery types was observed.

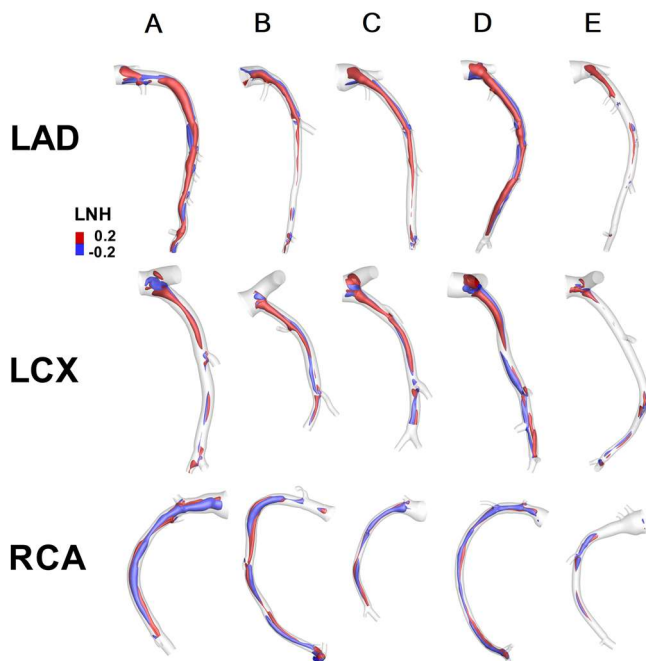


Figure 1. Investigated swine-specific coronary artery models. LNH averaged over the cardiac cycle is applied to visualize topological flow features (red (blue): right (left)-handed rotating helical structures).

Interestingly, it emerged that helicity intensity at baseline h_2 was associated with the percentage of surface area exposed to unfavourable shear conditions.

TABLE II

CORRELATION COEFFICIENTS FOR PERCENTAGE LUMINAL AREAS EXPOSE TO "DISTURBED SHEAR" VS. HELICITY INTENSITY

TAWSS33	OSI66	RRT66	transWSS66	CFI66
-0.93**	0.77**	-0.93**	0.88**	0.54*

* $p < 0.05$; ** $p < 0.01$;

In detail, h_2 was negatively associated with TAWSS33 (i.e. lower helicity intensity implies larger lumen area exposed to low WSS) and RRT66, and positively correlated to OSI66, transWSS66 and CFI66 percentage lumen areas (Table II). However, it must be reported that the threshold values (66th

percentile) identified for OSI (0.002), CFI (0.066) and transWSS (0.039 Pa) are very low, suggesting that WSS multidirectionality is not a feature marking out local hemodynamics in the 15 investigated coronary arteries.

From the analysis of WT at T2, it emerged that a low plaque growth per month was associated with high baseline levels of TAWSS and near-wall h_2 (Fig. 2). No significant associations emerged among plaque growth per month values and h_2 values integrated over the whole lumen of the vessel.

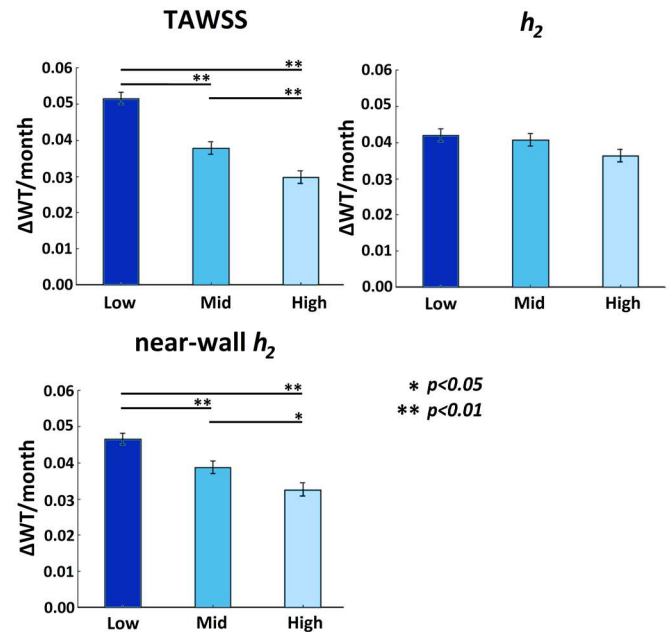


Figure 2. TAWSS, h_2 and near-wall h_2 vs. estimated plaque growth.

IV. CONCLUSION

Results from this study suggest that: (1) counter-rotating HF patterns naturally develop in coronary arteries and are negatively associated with descriptors of disturbed shear stress, suggesting a beneficial, atheroprotective role for HF in coronary arteries; (2) helicity intensity (h_2) is protective against WT and candidates as a potential biomechanical predictor of atherosclerotic plaque growth.

REFERENCES

- [1] U. Morbiducci, R. Ponzini, M. Grigioni, and A. Redaelli, "Helical flow as fluid dynamic signature for atherogenesis in aortocoronary bypass. A numeric study", *J. Biomech.*, vol. 40, pp. 519-534, 2007.
- [2] D. Gallo, P.B. Bijari, U. Morbiducci, Y. Qiao, Y. Xie, M. Etesami, D. Haabets, E.G. Lakatta, B.A. Wasserman, and D.A. Steinman, "Segment-specific associations between local haemodynamic and imaging markers of early atherosclerosis at the carotid artery: an in vivo human study", *J. R. Soc. Interface*, vol. 15(147), 2018.
- [3] A.G. van der Giessen, M. Schaap, F.J. Gijsen, H.C. Geoen, T. van Walsum, N.R. Mollet, J. Dijkstra, F. N. van de Vosse, W. J. Niessen, P. J. de Feyter, A.F.W. van der Steen, and J.J. Wentzel, "3D fusion of intravascular ultrasound and coronary computed tomography for in-vivo wall shear stress analysis: a feasibility study", *Int. J. Card. I.*, vol. 26, pp. 781-796, 2010.
- [4] Y. Huo, and G.S. Kassab, "Intraspecific scaling laws of vascular trees", *J. R. Soc. Interface*, vol. 9(66), pp. 190-200, 2012.
- [5] Y. Mohamied, S.J. Sherwin, and P.D. Weinberg, "Understanding the fluid mechanics behind transverse wall shear stress", *J. Biomech.*, vol. 50, pp. 102-109, 2017.
- [6] G. De Nisco, A.M. Kok, C. Chiastra, D. Gallo, A. Hoogendoorn, F. Migliavacca, J.J. Wentzel, and U. Morbiducci, "The atheroprotective nature of helical flow in coronary arteries", *Ann. Biomed. Eng.*, vol. 47(2), pp. 425-438, 2019.